Received: 10 January 2022 | Revised: 19 April 2022 | Accepted: 7 June 2022

DOI: 10.4218/etrij.2021-0485

ORIGINAL ARTICLE

ETRI Journal WILEY

Off-grid direction-of-arrival estimation for wideband noncircular sources

Xiaoyu Zhang[1] | Haihong Tao[1] | Ziye Fang[2] | Jian Xie[3]

[1]National Laboratory of Radar Signal Processing, Xidian University, Xi'an, China

[2]School of Computer Science and Technology, Xidian University, Xi'an, China

[3]School of Electronics and Information, Northwestern Polytechnical University, Xi'an, China

Correspondence
Xiaoyu Zhang, National Laboratory of Radar Signal Processing, Xidian University. Xi'an, China.
Email: xiaoyu_zhang_2020@qq.com

Funding information
Innovation Project of Science and Technology Commission of the Central Military Commission, Grant/Award Number: 19-HXXX-01-ZD-006-XXX-XX; National Key Laboratory Foundation, Grant/Award Number: 61424110302; National Natural Science Foundation of China, Grant/Award Number: 61771015

Abstract

Researchers have recently shown an increased interest in estimating the direction-of-arrival (DOA) of wideband noncircular sources, but existing studies have been restricted to subspace-based methods. An off-grid sparse recovery-based algorithm is proposed in this paper to improve the accuracy of existing algorithms in low signal-to-noise ratio situations. The covariance and pseudo covariance matrices can be jointly represented subject to block sparsity constraints by taking advantage of the joint sparsity between signal components and bias. Furthermore, the estimation problem is transformed into a single measurement vector problem utilizing the focused operation, resulting in a significant reduction in computational complexity. The proposed algorithm's error threshold and the Cramer–Rao bound for wideband noncircular DOA estimation are deduced in detail. The proposed algorithm's effectiveness and feasibility are demonstrated by simulation results.

KEYWORDS
array signal processing, direction-of-arrival estimation, off-grid, wideband noncircular signal

1 | INTRODUCTION

The field of array signal processing has a lot of interest in direction-of-arrival (DOA) estimation, which is widely used in radar, sonar, and wireless communications. Signals are supposed to be circularly symmetrical Gaussian distributed in traditional DOA estimation methods. However, in practice, amplitude modulated or binary phase-shift keying (BPSK) modulated signals are commonly used in telecommunications or satellite systems. Researchers have demonstrated that exploiting the noncircularity property of the signals can improve the performance of DOA algorithms over the last few decades. Gounon and others [1] were the first to extend the classical multiple signal classification (MUSIC) method to the noncircular-MUSIC (NC-MUSIC) method. In Chargé and others [2], the DOA estimation problem for noncircular sources was transformed into the polynomial rooting problem, and the NC-Root-MUSIC method was developed. Abeida and Delmas [3] examined the asymptotic performance of some MUSIC-like methods for noncircular DOA estimation. The improved algorithm was then used to estimate and identify a combination of noncircular and circular sources [4]. The researchers used a variety of methods to improve the estimation accuracy, including the high-order cumulant-based method [5] and the biquaternion-based method [6]. With a high signal-to-noise ratio (SNR) and sufficient snapshots, these

subspace-based algorithms can accurately estimate DOA for noncircular sources. The researchers have explored some sparse recovery (SR)-based algorithms to overcome the limitations of subspace-based algorithms since the development of compressed sensing theory and its widespread application in array signal processing. Liu and others [7] considered the noncircular covariance matrix sparse representation (NC-CMSR) method for noncircular DOA estimation through the joint sparse representation of the covariance and pseudo covariance matrices of incident signals. Similarly, Yang and others [8] estimated the signal subspace using a joint sparse reconstruction of two terms. Consequently, Cai and others [9] extended NC-CMSR to a coprime array. In addition, Zheng and others [10] developed a sparse Bayesian learning (SBL)-based algorithm for off-grid noncircular DOA estimation. On the other hand, all of the above DOA estimators are mostly limited to narrowband noncircular sources and cannot be used directly for wideband signals.

In a variety of practical applications, wideband signals are nearly ubiquitous. Previous studies about wideband DOA estimation methods can be categorized into three types: (a) maximum likelihood (ML) methods [11–13], (b) subspace-based algorithms [14–23], and (c) SR-based algorithms [24–30]. Multi-dimensional search is required by ML approaches, which are burdened by enormous computational complexities. On the other hand, subspace-based algorithms are more efficient. Several methods utilizing time-delayed samples have been developed in the time domain of wideband signals [14–16]. The incoherent signal subspace method (ISSM) [17] and the coherent signal subspace method (CSSM) [18] are two frequency schemes. CSSM often uses the focusing operation to align the signal subspace and concentrate the dispersed energy at different frequency bins [21–23], whereas ISSM typically employs narrowband signal processing methods for each frequency bin [19,20].

The theory of compressed sensing has also been widely used in wideband DOA estimation. The difference from the SR-based narrowband methods is that the joint sparsity of wideband sources should be taken into account. Because of the disparity of array manifold matrices at different frequency bins, previous research has primarily focused on three ideas for building the sparse wideband signal model. To avoid the array manifold matrices corresponding to different frequency bins, the over complete dictionary could be constructed using the correlation function of the signals [24]. On the other hand, the correlation function can only be calculated in a few specific scenarios. The second idea is to formulate the wideband signal as a block SR problem [25–27]. Although the dictionary contains array manifold matrices at all frequency bins, the dictionary's large size may result in enormous computational complexity. The third idea is to transform the signal model into the multiple measurement vectors (MMV) problem [28–30]. Different manifold matrices can be concentrated into a single dictionary. Because the dictionary is smaller, MMV-based methods are more efficient than the block sparse-based approaches.

A few studies on noncircular wideband DOA estimation have recently been performed. Based on the baseband form of the steering technique [31], time-delayed array snapshot vector was considered in Huang and others [32] to align the wideband noncircular signal. Some algorithms, such as the envelope aligned inverse power (EAIP) method [32], the complex envelope aligned rank-reduction (EARR) method [33], and the aligned propagator method (APM) [34], have been developed based on this conceptual framework to realize noncircular wideband DOA estimation. Yang and others [35] extended the method in Gou and others [6] and proposed the wideband biquaternion noncircular cumulant (WBNC) method to process the non-Gaussian and noncircular wideband sources. Existing noncircular wideband DOA estimators share the same flaws as subspace-based methods; a priori information of source number is required, and the performance degrades at low SNR. Furthermore, for the multipath signal model, these methods underperform.

To address these issues, the compressive sensing theory is used for the first time in this paper to solve the wideband noncircular DOA estimation problem, and the focused based off-grid wideband noncircular (FOGWNC) DOA estimation algorithm is proposed. First and foremost, a novel signal model for multipath noncircular wideband signals is proposed in the frequency domain. After preprocessing with Taylor expansion, noise reduction, and dictionary focusing, two single measurement vector problems are formulated. The covariance and pseudo covariance matrices can be jointly represented subject to block sparsity constraints, taking advantage of the joint sparsity between signal components and bias. Finally, convex optimization can be used to obtain results. The proposed method does not require source number. In low SNR, simulation results show that FOGWNC can efficiently address noncircular wideband DOA estimation and obtain more accurate results than existing subspace-based methods [32–35]. In addition, the proposed algorithm's error thresholds and the Cramer–Rao bound (CRB) for wideband noncircular DOA estimation are deduced in detail.

The remainder of this paper is organized in the following manner: In section 2, the multipath wideband noncircular signal model for sparse reconstruction is

studied. In section 3, the off-grid model is introduced, followed by the FOGWNC algorithm. In section 4, simulation is used to compare the performance and computational time of various algorithms. The following notations are used in this paper. $(\cdot)^*$, $(\cdot)^{\mathrm{T}}$, and $(\cdot)^{\mathrm{H}}$ are mean conjugation, transposition, and conjugation transposition, respectively. $\Re(\cdot)$ and $\Im(\cdot)$ mean the real and the imaginary parts. blkdiag$(\cdot)$ and vec$(\cdot)$ denote the block diagonal matrix and the vectorization operator, respectively. diag$(\cdot)$ means diagonal matrix or diagonals of a matrix. $\|\cdot\|$ represents the matrix norm. $\otimes$, $\odot$, and $\circ$ mean the Kronecker product, Khatri–Rao product, and Hadamard product, respectively. $\mathbf{O}$ is the zero matrix, and $\mathbf{I}$ is the identity matrix.

2 | PROBLEM FORMULATION

Suppose that K_{nc} signals from K far-field independent wideband noncircular sources impinging on the linear array with M sensors from different directions. Each signal can be divided into P_k groups, which means that $K_{\mathrm{nc}} = \sum_{k=1}^{K} P_k$. The demodulated output baseband signal of the mth sensor can be formulated as

$$y_m(t) = \sum_{k=1}^{K}\sum_{i=1}^{P_k} \rho_{ki} s_k(t + \tau_{m,\theta_{ki}} + \iota_{ki}) e^{j2\pi f_0\left(\tau_{m,\theta_{ki}} + \iota_{ki}\right)} + n_m(t), \tag{1}$$

where θ_{ki} denotes the direction of the signal from the kth source and the ith path. $s_k(t)$ is the zero-mean complex envelope of the kth line-of-sight (LOS) wideband signal, and $n_m(t)$ is the circular additive noise with the mth sensor. f_0 is the carrier frequency, $\tau_{m,\theta_{ki}} = d_m \sin\theta_{ki}/c$ denotes the propagation delay of kith signal, and d_m is the distance between the mth sensor and the reference point c and represents the speed of propagation. ρ_{ki} and ι_{ki} are the attenuation factor and multipath propagation delay, respectively. The multipath delay is assumed to be no less than the correlation time, implying that the multipath signals are roughly uncorrelated with the LOS signal. For noncircular signals, it can be verified that $\mathrm{E}\{s_k^2(t)\} = \varsigma_k e^{j\phi_k}\mathrm{E}\{|s_k(t)|^2\}$, where ς_k and ϕ_k are the noncircularity rate and noncircularity phase, respectively. After sampling with f_s, the output vector in the time domain is divided into Q nonoverlapping groups with the same length L. The baseband signal in the frequency domain can be deduced through the discrete Fourier transform [32], that is,

$$\begin{aligned}\mathbf{Y}[l,q] &= \mathbf{A}(\boldsymbol{\theta},l)\mathbf{B}[l]\boldsymbol{\Gamma}\mathbf{S}[l,q] + \mathbf{N}[l,q] \\ &= \mathbf{A}(\boldsymbol{\theta},l)\mathbf{X}[l,q] + \mathbf{N}[l,q],\end{aligned} \tag{2}$$

where $\mathbf{S}[l,q]$ and $\mathbf{N}[l,q]$ mean the signal and noise vector corresponding to the lth frequency bin and the qth segment, respectively. $\mathbf{X}[l,q] = \mathbf{B}[l]\boldsymbol{\Gamma}\mathbf{S}[l,q]$ can be regarded as the signal components to be estimated. $\mathbf{A}(\boldsymbol{\theta},l)$ is the array manifold with the lth frequency bin, and $\mathbf{B}[l]$ and $\boldsymbol{\Gamma}$ contain the information of attenuation factor and multipath propagation delay, respectively. The above matrix can be formulated as follows:

$$\begin{aligned}\mathbf{A}(\boldsymbol{\theta},l) &= [\mathbf{A}_1(\boldsymbol{\theta},l),\ \mathbf{A}_2(\boldsymbol{\theta},l),\ \cdots,\ \mathbf{A}_K(\boldsymbol{\theta},l)], \\ \mathbf{A}_k(\boldsymbol{\theta},l) &= [\mathbf{a}(k1,l),\ \mathbf{a}(k2,l),\ \cdots,\ \mathbf{a}(kP_k,l)], \\ \mathbf{a}(ki,l) &= \left[e^{j2\pi(f_l+f_0)\tau_{1,\theta_{ki}}},\ e^{j2\pi(f_l+f_0)\tau_{2,\theta_{ki}}},\ \cdots,\ e^{j2\pi(f_l+f_0)\tau_{M,\theta_{ki}}}\right]^{\mathrm{T}}, \\ \mathbf{B}[l] &= \mathrm{blkdiag}(\mathbf{B}_1[l],\ \mathbf{B}_2[l],\ \cdots,\ \mathbf{B}_K[l]), \\ \mathbf{B}_k[l] &= \mathrm{diag}\left(e^{j2\pi(f_l+f_0)\iota_{\theta_{k1}}},\ e^{j2\pi(f_l+f_0)\iota_{\theta_{k2}}},\ \cdots,\ e^{j2\pi(f_l+f_0)\iota_{\theta_{kP_k}}}\right), \\ \boldsymbol{\Gamma} &= \mathrm{blkdiag}(\boldsymbol{\rho}_1,\ \boldsymbol{\rho}_2,\ \cdots,\ \boldsymbol{\rho}_K),\ \boldsymbol{\rho}_k = \left[\rho_{k1},\ \rho_{k2},\ \cdots,\ \rho_{kP_k}\right]^{\mathrm{T}}.\end{aligned} \tag{3}$$

It is worth noting that the frequency bins of wideband sources with bandwidth B are distributed between the lowest frequency $f_0 - B/2$ and the highest frequency in most previous studies. In contrast to the traditional model for wideband circular sources, $\boldsymbol{S}[l,q]$ is located between $-B/2$ and $B/2$ in the frequency domain, and f_l means the lth frequency bin of the baseband signal. In other words, the frequency bins in (2) that correspond to the steering vector and the signal's frequency bins are not the same. The array output covariance matrix and the pseudo covariance matrix of each frequency bin can be estimated from limited snapshots in practice applications, that is

$$\begin{aligned}\widehat{\mathbf{R}}_{\mathrm{c}}[l] &= \frac{1}{Q}\sum_{q=0}^{Q-1}\mathbf{Y}[l,q]\cdot\mathbf{Y}^{\mathrm{H}}[l,q], \\ \widehat{\mathbf{R}}_{\mathrm{nc}}[l] &= \frac{1}{Q}\sum_{q=0}^{Q-1}\mathbf{Y}[l,q]\cdot\mathbf{Y}^{\mathrm{T}}[l,q].\end{aligned} \tag{4}$$

This paper $\iota_{ki_1} - \iota_{ki_2}(i_1 \neq i_2)$ is supposed to be large enough that different multipath signals from the same source are approximately uncorrelated from each other. Based on this assumption, the covariance matrices can be vectorized as

$$\begin{aligned}\mathbf{r}_{\mathrm{c}}[l] &= \mathrm{vec}(\mathbf{R}_{\mathrm{c}}[l]) = (\mathbf{A}^*(\boldsymbol{\theta},l)\ \odot\ \boldsymbol{A}(\boldsymbol{\theta},l))\boldsymbol{\gamma}_{\mathrm{c}}[l] + \sigma_2^1\mathbf{i}_{M^2} \\ \mathbf{r}_{\mathrm{nc}}[l] &= \mathrm{vec}(\mathbf{R}_{\mathrm{nc}}[l]) = (\mathbf{A}(\boldsymbol{\theta},l)\ \odot\ \mathbf{A}(\boldsymbol{\theta},l))\boldsymbol{\gamma}_{\mathrm{nc}}[l],\end{aligned} \tag{5}$$

where $\mathbf{i}_{M^2} = \mathrm{vec}(\mathbf{I}_M)$ and

$$\begin{aligned}\boldsymbol{\gamma}_{\mathrm{c}}[l] &= [\gamma_{\mathrm{c}}[11,l], ..., \gamma_{\mathrm{c}}[kP_k,l], ..., \gamma_{\mathrm{c}}[KP_K,l]]^{\mathrm{T}},\\ \boldsymbol{\gamma}_{\mathrm{nc}}[l] &= [\gamma_{\mathrm{nc}}[11,l], ..., \gamma_{\mathrm{nc}}[kP_k,l], ..., \gamma_{\mathrm{nc}}[KP_K,l]]^{\mathrm{T}}.\end{aligned} \tag{6}$$

Notably, $\gamma_{\mathrm{c}}[ki,l] \neq \gamma_{\mathrm{nc}}[ki,l]$. $\gamma_{\mathrm{c}}[ki,l]$ is the power of the ki th entry in $\mathbf{X}[l,q]$, and $\gamma_{\mathrm{nc}}[ki,l]$ contains the noncircular information from the pseudo covariance matrix.

3 | PROBLEM FORMULATION

For wideband noncircular sources, a novel off-grid DOA estimation algorithm is proposed in this section.

3.1 | Off-grid model for each frequency bin

It is obvious that the noise component only exists in diagonal elements of the covariance matrix $\mathbf{R}_{\mathrm{c}}[l]$. Noise can be reduced at the expense of degree-of-freedom to improve performance. The selecting matrix $\mathbf{J}$ is defined as $\mathbf{J} = [\mathbf{J}_1, \mathbf{J}_2, ..., \mathbf{J}_{M-1}]^{\mathrm{T}}$, where $\mathbf{J}_m = \left[\bar{e}_{m(M+1)-M+1}, ..., \bar{e}_{m(M+1)}\right]$ and $\bar{e}_i$ is an all-zero vector except the element at ith index is one. The observation vector can be formulated by vectorizing the covariance matrix after the noise reduction preprocess:

$$\begin{aligned}\mathbf{y}_{\mathrm{c}}[l] &= \mathbf{J}\cdot\mathrm{vec}(\mathbf{R}_{\mathrm{c}}[l]) = \mathbf{J}\mathbf{A}_{\mathrm{c}}(\boldsymbol{\theta},l)\boldsymbol{\gamma}_{\mathrm{c}}[l],\\ \mathbf{y}_{\mathrm{nc}}[l] &= \mathbf{A}_{\mathrm{nc}}(\boldsymbol{\theta},l)\boldsymbol{\gamma}_{\mathrm{nc}}[l],\end{aligned} \tag{7}$$

where $\mathbf{y}_{\mathrm{nc}}[l] = \mathbf{r}_{\mathrm{nc}}[l]$ is the virtually noncircular signal vector. The array manifold can be expressed as

$$\begin{aligned}\mathbf{A}_{\mathrm{c}}(\boldsymbol{\theta},l) &= \mathbf{A}^{*}(\boldsymbol{\theta},l) \odot \mathbf{A}(\boldsymbol{\theta},l) = [\mathbf{a}_{\mathrm{c}}(11,l), ..., \mathbf{a}_{\mathrm{c}}(KP_K,l)],\\ \mathbf{A}_{\mathrm{nc}}(\boldsymbol{\theta},l) &= \mathbf{A}(\boldsymbol{\theta},l) \odot \mathbf{A}(\boldsymbol{\theta},l) = [\mathbf{a}_{\mathrm{nc}}(11,l), ..., \mathbf{a}_{\mathrm{nc}}(KP_K,l)].\end{aligned} \tag{8}$$

In traditional SR-based on-grid methods, the incident signal is supposed to be uniformly distributed in K_g the predefined grid $\widetilde{\boldsymbol{\theta}} = \{\theta_1, \theta_2, ..., \theta_{K_g}\}$. The observation model can be denoted as

$$\mathbf{y}_{\mathrm{c}}[l] = \mathbf{J}\mathbf{A}_{\mathrm{c}}\left(\widetilde{\boldsymbol{\theta}},l\right)\boldsymbol{\gamma}_{\mathrm{c}}^{\circ}[l],\ \mathbf{y}_{\mathrm{nc}}[l] = \mathbf{A}_{\mathrm{nc}}\left(\widetilde{\boldsymbol{\theta}},l\right)\boldsymbol{\gamma}_{\mathrm{nc}}^{\circ}[l], \tag{9}$$

where $(\cdot)^{\circ}$ means the entries corresponding to the grid. Suppose that θ_{ki} is the real direction, for $k_g \in \{1, 2, \cdots, K_g\}$, we have

$$\boldsymbol{\gamma}_{\mathrm{c}}^{\circ}[l] = \begin{cases}\gamma_{\mathrm{c}}[ki,l], & \theta_{k_g} = \theta_{ki},\\ 0, & \theta_{k_g} \neq \theta_{ki},\end{cases}\quad \boldsymbol{\gamma}_{\mathrm{nc}}^{\circ}[l] = \begin{cases}\gamma_{\mathrm{nc}}[ki,l], & \theta_{k_g} = \theta_{ki},\\ 0, & \theta_{k_g} \neq \theta_{ki}.\end{cases} \tag{10}$$

The grid is always set to be dense enough to ensure the accuracy of DOA estimation, but the prohibitive computational complexity restricts the development of on-grid methods. Furthermore, in practice, the true angle is unlikely to be exactly on the grid. The off-grid model has been widely researched in recent years to overcome the problem caused by the model mismatch. Suppose that κ_g is the nearest index to ki and $r = \theta_2 - \theta_1$ is the step size of the original uniform grid. Using Taylor expansion θ_{κ_g}, the steering vector associated with the predefined grid of each frequency bin can be approximated and formulated as

$$\begin{aligned}\mathbf{a}_{\mathrm{c}}(ki,l) &\approx \mathbf{a}_{\mathrm{c}}(\kappa_g,l) + \mathbf{a}_{\mathrm{c}}'(\kappa_g,l)(\theta_{ki} - \theta_{\kappa_g}),\\ \mathbf{a}_{\mathrm{nc}}(ki,l) &\approx \mathbf{a}_{\mathrm{nc}}(\kappa_g,l) + \mathbf{a}_{\mathrm{nc}}'(\kappa_g,l)(\theta_{ki} - \theta_{\kappa_g}),\end{aligned} \tag{11}$$

where

$$\mathbf{a}_{\mathrm{c}}'(\kappa_g,l) = \frac{\partial \mathbf{a}_{\mathrm{c}}(\kappa_g,l)}{\partial \theta_{\kappa_g}},\ \mathbf{a}_{\mathrm{nc}}'(\kappa_g,l) = \frac{\partial \mathbf{a}_{\mathrm{nc}}(\kappa_g,l)}{\partial \theta_{\kappa_g}}. \tag{12}$$

Denote the derivative matrix related to the grid as

$$\begin{aligned}\mathbf{A}_{\mathrm{c}}'\left(\widetilde{\boldsymbol{\theta}},l\right) &= [\mathbf{a}_{\mathrm{c}}'(1,l), ..., \mathbf{a}_{\mathrm{c}}'(K_g,l)],\\ \mathbf{A}_{\mathrm{nc}}'\left(\widetilde{\boldsymbol{\theta}},l\right) &= [\mathbf{a}_{\mathrm{nc}}'(1,l), ..., \mathbf{a}_{\mathrm{nc}}'(K_g,l)].\end{aligned} \tag{13}$$

Each frequency bin shares the same bias $\boldsymbol{\alpha} = [\alpha_1, ..., \alpha_{K_g}]^{\mathrm{T}}$ and the corresponding matrix $\boldsymbol{\Delta} = \mathrm{diag}\{\boldsymbol{\alpha}\}$, where

$$\alpha_{k_g} = \begin{cases}\theta_{ki} - \theta_{\kappa_g}, & k_g = \kappa_g\\ 0, & k_g \neq \kappa_g\end{cases}. \tag{14}$$

The model (9) can be redefined as

$$\begin{aligned}\mathbf{y}_{\mathrm{c}}[l] &\approx \mathbf{J}\left(\mathbf{A}_{\mathrm{c}}\left(\widetilde{\boldsymbol{\theta}},l\right) + \mathbf{A}_{\mathrm{c}}'\left(\widetilde{\boldsymbol{\theta}},l\right)\boldsymbol{\Delta}\right)\boldsymbol{\gamma}_{\mathrm{c}}^{\circ}[l],\\ \mathbf{y}_{\mathrm{nc}}[l] &\approx \left(\mathbf{A}_{\mathrm{nc}}\left(\widetilde{\boldsymbol{\theta}},l\right) + \mathbf{A}_{\mathrm{nc}}'\left(\widetilde{\boldsymbol{\theta}},l\right)\boldsymbol{\Delta}\right)\boldsymbol{\gamma}_{\mathrm{nc}}^{\circ}[l].\end{aligned} \tag{15}$$

3.2 | FOGWNC algorithm

The focused operation is applied for the off-grid model in this subsection to reduce computational complexity and improve accuracy. The rotational signal subspace operation can be used to reduce the error between the array manifold focused by each frequency bin and the array manifold of the reference frequency bin. In other words, the reference frequency band's signal components are all aligned to the reference frequency bin, that is,

$$\min_{\mathbf{T}(l)} \|\mathbf{A}(\boldsymbol{\theta},l_{\mathrm{r}})-\mathbf{T}_l\mathbf{A}(\boldsymbol{\theta},l)\|_{\mathrm{F}} \;\; s.t. \;\; \mathbf{T}_l^{\mathrm{H}}\mathbf{T}_l=\mathbf{I}, \tag{16}$$

where $\mathbf{T}_l$ is the focusing matrix corresponding to the lth frequency bin, and l_{r} is the index of reference frequency point. One particular solution of (16) is $\mathbf{T}_l=\mathbf{U}_l\mathbf{V}_l^{\mathrm{H}}$. $\mathbf{U}_l$ and $\mathbf{V}_l$ are the left singular matrix and right singular matrix of $\mathbf{A}(\boldsymbol{\theta},l)\mathbf{A}^{\mathrm{H}}(\boldsymbol{\theta},l_{\mathrm{r}})$, respectively. From the property of singular value decomposition, $\mathbf{U}_l$ and $\mathbf{V}_l$ are unitary matrices. Let $\mathbf{R}_{\mathrm{rc}}$ and $\mathbf{R}_{\mathrm{rnc}}$ be the focused covariance matrix and pseudo covariance matrix. The novel vectorized models are given by

$$\begin{aligned}
\mathbf{r}_{\mathrm{rc}}&=\mathrm{vec}(\mathbf{R}_{\mathrm{rc}})=\mathrm{vec}\left(\frac{1}{L}\sum_{l=1}^{L}\mathbf{T}_l\mathbf{R}_{\mathrm{c}}[l]\mathbf{T}_l^{\mathrm{H}}\right)\\
&=\frac{1}{L}\sum_{l=1}^{L}\left(\mathbf{T}_l^{*}\otimes\mathbf{T}_l\right)[\mathbf{A}^{*}(\boldsymbol{\theta},l)\odot\mathbf{A}(\boldsymbol{\theta},l)]\boldsymbol{\gamma}_{\mathrm{c}}[l]\\
&\quad+\frac{1}{L}\sum_{l=1}^{L}\left(\mathbf{T}_l^{*}\otimes\mathbf{T}_l\right)\sigma_l^2\mathbf{i}_{M^2}=\frac{1}{L}\sum_{l=1}^{L}\left[\mathbf{T}_l^{*}\mathbf{A}^{*}(\boldsymbol{\theta},l)\odot\mathbf{T}_l\mathbf{A}(\boldsymbol{\theta},l)\right]\boldsymbol{\gamma}_{\mathrm{c}}[l]\\
&\quad+\frac{1}{L}\sum_{l=1}^{L}\sigma_l^2\mathrm{vec}\left(\mathbf{U}_l\mathbf{V}_l^{\mathrm{H}}\mathbf{V}_l\mathbf{U}_l^{\mathrm{H}}\right)\approx[\mathbf{A}^{*}(\boldsymbol{\theta},l_{\mathrm{r}})\odot\mathbf{A}(\boldsymbol{\theta},l_{\mathrm{r}})]\cdot\frac{1}{L}\sum_{l=1}^{L}\boldsymbol{\gamma}_{\mathrm{c}}[l]\\
&\quad+\frac{1}{L}\sum_{l=1}^{L}\sigma_l^2\cdot\mathrm{vec}(\mathbf{I})=\mathbf{A}_{\mathrm{c}}(\boldsymbol{\theta},l_{\mathrm{r}})\overline{\boldsymbol{\gamma}}_{\mathrm{c}}+\overline{\sigma}^2\mathbf{i}_{M^2},\\
\mathbf{r}_{\mathrm{rnc}}&=\mathrm{vec}(\mathbf{R}_{\mathrm{rnc}})=\mathrm{vec}\left(\frac{1}{L}\sum_{l=1}^{L}\mathbf{T}_l\mathbf{R}_{\mathrm{nc}}[l]\mathbf{T}_l^{\mathrm{T}}\right)\\
&=\frac{1}{L}\sum_{l=1}^{L}(\mathbf{T}_l\otimes\mathbf{T}_l)(\mathbf{A}(\boldsymbol{\theta},l)\odot\mathbf{A}(\boldsymbol{\theta},l))\boldsymbol{\gamma}_{\mathrm{nc}}[l]\\
&=\frac{1}{L}\sum_{l=1}^{L}[\mathbf{T}_l\mathbf{A}(\boldsymbol{\theta},l)\odot\mathbf{T}_l\mathbf{A}(\boldsymbol{\theta},l)]\boldsymbol{\gamma}_{\mathrm{nc}}[l]\approx\mathbf{A}_{\mathrm{nc}}(\boldsymbol{\theta},l_{\mathrm{r}})\overline{\boldsymbol{\gamma}}_{\mathrm{nc}},
\end{aligned} \tag{17}$$

where $\overline{\boldsymbol{\gamma}}_{\mathrm{c}}$ and $\overline{\boldsymbol{\gamma}}_{\mathrm{nc}}$ are vectors consisting of the average power of all frequency bins, that is,

$$\begin{aligned}
\overline{\boldsymbol{\gamma}}_{\mathrm{c}}&=\frac{1}{L}\sum_{l=1}^{L}\boldsymbol{\gamma}_{\mathrm{c}}[l]=[\overline{\gamma}_{\mathrm{c}}(11),\cdots,\overline{\gamma}_{\mathrm{c}}(kP_k),\cdots,\overline{\gamma}_{\mathrm{c}}(KP_K)]^{\mathrm{T}},\\
\overline{\boldsymbol{\gamma}}_{\mathrm{nc}}&=\frac{1}{L}\sum_{l=1}^{L}\boldsymbol{\gamma}_{\mathrm{nc}}[l]=[\overline{\gamma}_{\mathrm{nc}}(11),\cdots,\overline{\gamma}_{\mathrm{nc}}(kP_k),\cdots,\overline{\gamma}_{\mathrm{nc}}(KP_K)]^{\mathrm{T}}.
\end{aligned} \tag{18}$$

$\overline{\sigma}^2$ is the average variance of noise across the whole band. The observation vectors can be expressed as

$$\begin{aligned}
\mathbf{y}_{\mathrm{rc}}&=\mathbf{J}\mathbf{A}_{\mathrm{c}}(\boldsymbol{\theta},l_{\mathrm{r}})\overline{\boldsymbol{\gamma}}_{\mathrm{c}},\\
\mathbf{y}_{\mathrm{rnc}}&=\mathbf{A}_{\mathrm{nc}}(\boldsymbol{\theta},l_{\mathrm{r}})\overline{\boldsymbol{\gamma}}_{\mathrm{nc}}.
\end{aligned} \tag{19}$$

The sparse reconstruction problems are

$$\begin{aligned}
&\min\ \|\overline{\boldsymbol{\gamma}}_{\mathrm{c}}^{\circ}\|_0\ \ \text{s.t. }\mathbf{y}_{\mathrm{rc}}=\boldsymbol{J}\boldsymbol{A}_{\mathrm{c}}\left(\widetilde{\boldsymbol{\theta}},l_{\mathrm{r}}\right)\overline{\boldsymbol{\gamma}}_{\mathrm{c}}^{\circ},\\
&\min\ \|\overline{\boldsymbol{\gamma}}_{\mathrm{nc}}^{\circ}\|_0\ \ \text{s.t. }\mathbf{y}_{\mathrm{rnc}}=\boldsymbol{A}_{\mathrm{nc}}\left(\widetilde{\boldsymbol{\theta}},l_{\mathrm{r}}\right)\overline{\boldsymbol{\gamma}}_{\mathrm{nc}}^{\circ},
\end{aligned} \tag{20}$$

where $\overline{\boldsymbol{\gamma}}_{\mathrm{c}}^{\circ}$ and $\overline{\boldsymbol{\gamma}}_{\mathrm{nc}}^{\circ}$ denote the average power related to the grids. The dictionary's dimension is greatly reduced in comparison to the MMV model of all frequency bins. The over complete dictionaries are $\mathbf{J}\mathbf{A}_{\mathrm{c}}(\widetilde{\boldsymbol{\theta}},l_{\mathrm{r}})$ and $\mathbf{A}_{\mathrm{nc}}(\widetilde{\boldsymbol{\theta}},l_{\mathrm{r}})$, and the related derivative matrices are $\mathbf{J}\mathbf{A}_{\mathrm{c}}'(\widetilde{\boldsymbol{\theta}},l_r)$ and $\mathbf{A}_{\mathrm{nc}}'(\widetilde{\boldsymbol{\theta}},l_{\mathrm{r}})$. Denote $\boldsymbol{\alpha}_{\mathrm{c}}^{\circ}=\boldsymbol{\alpha}\circ\overline{\boldsymbol{\gamma}}_{\mathrm{c}}^{\circ}$, $\boldsymbol{\gamma}_{\mathrm{r}}^{\circ}=\left[\gamma_{\mathrm{r}}(1),\ldots,\gamma_{\mathrm{r}}\left(K_g\right)\right]^{\mathrm{T}}$, and $\Upsilon=\left[\boldsymbol{\gamma}_{\mathrm{r}}^{\circ},\overline{\boldsymbol{\gamma}}_{\mathrm{c}}^{\circ},\overline{\boldsymbol{\gamma}}_{\mathrm{nc}}^{\circ},\boldsymbol{\alpha}_{\mathrm{c}}^{\circ}\right]$. To combine the angle information contained in both the covariance matrix and the pseudo covariance matrix, (20) can be transformed as a convex problem:

$$\begin{aligned}
&\min_{\boldsymbol{\gamma}_{\mathrm{r}}^{\circ},\overline{\boldsymbol{\gamma}}_{\mathrm{c}}^{\circ},\overline{\boldsymbol{\gamma}}_{\mathrm{nc}}^{\circ},\boldsymbol{\alpha}_{\mathrm{c}}^{\circ}}\ \|\Upsilon\|_{2,1}\\
&\text{s.t. }\gamma_{\mathrm{r}}(k_g)\geq\left\|\left[\overline{\gamma}_{\mathrm{c}}(k_g),\overline{\gamma}_{\mathrm{nc}}(k_g)\right]\right\|_2\\
&\left\|\mathbf{y}_{\mathrm{rc}}-\mathbf{J}\mathbf{A}_{\mathrm{c}}\left(\widetilde{\boldsymbol{\theta}},l_{\mathrm{r}}\right)\overline{\boldsymbol{\gamma}}_{\mathrm{c}}^{\circ}-\mathbf{A}_{\mathrm{nc}}'\left(\widetilde{\boldsymbol{\theta}},l_{\mathrm{r}}\right)\boldsymbol{\alpha}_{\mathrm{c}}^{\circ}\right\|_2\leq\varepsilon_{\mathrm{c}},\\
&\left\|\mathbf{y}_{\mathrm{rnc}}-\mathbf{A}_{\mathrm{nc}}\left(\widetilde{\boldsymbol{\theta}},l_{\mathrm{r}}\right)\overline{\boldsymbol{\gamma}}_{\mathrm{nc}}^{\circ}\right\|_2\leq\varepsilon_{\mathrm{nc}}\\
&-\frac{r}{2}\overline{\boldsymbol{\gamma}}_{\mathrm{c}}^{\circ}\preceq\boldsymbol{\alpha}_{\mathrm{c}}^{\circ}\preceq\frac{r}{2}\overline{\boldsymbol{\gamma}}_{\mathrm{c}}^{\circ}
\end{aligned} \tag{21}$$

where $\|\Upsilon\|_{2,1}=\sum_{k=1}^{K_g}\|\Upsilon(k,:)\|_2$. Taking advantage of the joint sparsity between $\boldsymbol{\gamma}_{\mathrm{r}}^{\circ}$, $\overline{\boldsymbol{\gamma}}_{\mathrm{c}}^{\circ}$, $\overline{\boldsymbol{\gamma}}_{\mathrm{nc}}^{\circ}$, and $\boldsymbol{\alpha}_{\mathrm{c}}^{\circ}$, the DOA information from the covariance matrix and the pseudo covariance matrix is aligned $\boldsymbol{\gamma}_{\mathrm{r}}^{\circ}$. The error bound ε_{c} $\varepsilon_{\mathrm{nc}}$ directly affects the accuracy of the result; thus, the thresholds should be determined before solving the problem. Assuming that $\widehat{\mathbf{R}}_{\mathrm{rc}\_m_1,m_2}$ and $\widehat{\mathbf{R}}_{\mathrm{rnc}\_m_1,m_2}$ are the elements of m_1th row and m_2th column in $\widehat{\mathbf{R}}_{\mathrm{rc}}$ and $\widehat{\mathbf{R}}_{\mathrm{rnc}}$, respectively, the error can be formulated as

$$\varepsilon_{\mathrm{c}} \approx \mu_{\mathrm{c}} \left[-\frac{M(M-1)}{Q} \sum_{k=1}^{K} \sum_{i=1}^{P_k} \left(\overline{\gamma}_{\mathrm{c}}^2(ki) + \overline{\gamma}_{\mathrm{nc}}^2(ki) \right) + \frac{M(M-1)}{Q} \left(\overline{\sigma}^2 + \sum_{k=1}^{K} \sum_{i=1}^{P_k} \overline{\gamma}_{\mathrm{c}}(ki) \right)^2 + \frac{1}{Q} \sum_{m_1=1}^{M} \sum_{\substack{m_2=1 \\ m_2 \neq m_1}}^{M} \left| \widehat{\mathbf{R}}_{\mathrm{rnc}_{m_1,m_2}} \right|^2 \right]$$

$$\varepsilon_{\mathrm{nc}} \approx \mu_{\mathrm{nc}} \left[\frac{M(M+1)}{Q} \left(\overline{\sigma}^2 + \sum_{k=1}^{K} \sum_{i=1}^{P_k} \overline{\gamma}_{\mathrm{c}}(ki) \right)^2 + \frac{1}{Q} \sum_{m_1=1}^{M} \sum_{\substack{m_2=1 \\ m_2 \neq m_1}}^{M} \left| \widehat{\mathbf{R}}_{\mathrm{rc\_}m_1,m_2} \right|^2 - \frac{2M^2}{Q} \sum_{k=1}^{K} \sum_{i=1}^{P_k} \overline{\gamma}_{\mathrm{c}}^2(ki) \right]^{\frac{1}{2}}, \tag{22}$$

where μ_{c} and μ_{nc} are the empirical weight parameters; the detailed derivation can be found in Appendix A. In practice, $\overline{\sigma}^2 + \sum_{k=1}^{K} \sum_{i=1}^{P_k} \overline{\gamma}_{\mathrm{c}}(ki)$ can be estimated by diagonal elements of $\widehat{\mathbf{R}}_{\mathrm{rc}}$. $\sum_{k=1}^{K} \sum_{i=1}^{P_k} \overline{\gamma}_{\mathrm{c}}^2(ki)$ and $\sum_{k=1}^{K} \sum_{i=1}^{P_k} \overline{\gamma}_{\mathrm{nc}}^2(ki)$ can be calculated by the average of the square sum of the entries in $\|\mathbf{y}_{\mathrm{rc}}\|_2^2$ and $\|\mathbf{y}_{\mathrm{rnc}}\|_2^2$, respectively.

4 | SIMULATION RESULTS

Simulation results are presented in this section to demonstrate the proposed algorithm's performance. The same computer, with an AMD R7-4800H CPU and 16 GB of RAM, is used to simulate all of the results, which is running MATLAB R2020a on a 64-bit Windows 10 system. The proposed algorithm is compared to almost all the DOA estimation methods for wideband noncircular signals, including EAIP [32], EARR [33], APM [34], and WBNC [35]. The standard off-grid method based on sparse Bayesian inference [36] and the sparse Bayesian learning off-grid DOA estimation with Gaussian mixture priors [10] are also compared. It is worth noting that these two narrowband DOA estimators can only be used on individual frequency bins of wideband signals. For the sake of fairness, the step size is set as 1° within $(-90°, 90°)$ for off-grid methods and 0.1° the other subspace-based algorithms.

In the first case, two groups of four off-grid BPSK wideband signals impinge onto the six elements minimum-redundancy linear array [37] located at $(0, d, 2d, 6d, 10d, 13d)$ from $(-42.5°, -21.2°)$ and $(20.3°, 25.8°)$. The LOS signal is the first in each group, followed by the multipath signal. The noncircularity phase of two LOS signals is 50° and 70°. The multipath propagation delays $\iota_{12} = T_{\mathrm{c}}$, $\iota_{22} = 1.2T_{\mathrm{c}}$ and the attenuation factors $\rho_{12} = 0.8e^{j57.2°}$, $\rho_{22} = 0.9e^{j82.3°}$, where T_{c} is the correlation time. The element spacing d equals the half wavelength at the highest frequency. The carrier frequency is 2 GHz, and the bandwidth is 400 MHz, which is 20% of the center frequency. The sampling frequency is 5 GHz. SNR = 0 dB, the number of snapshots $N = 5000$, the number of subbands $L = 50$, and the number of segments $Q = N/L$. The scanning angle range is set as the prediction angle range of the focusing operation in FOGWNC. Figure 1. depicts the results. Existing subspace-based algorithms and the SBL-based off-grid methods produce far more false peaks than the proposed algorithm.

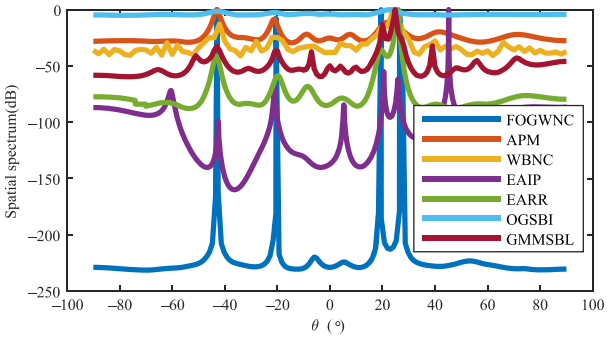

FIGURE 1 Spatial spectra of the compared methods

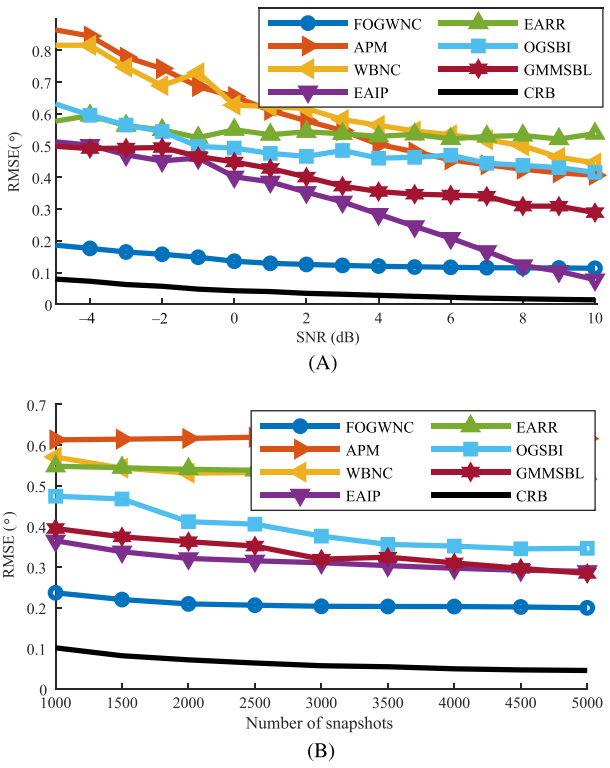

FIGURE 2 RMSE. (A) RMSE versus SNR for noncircular signals. (B) RMSE versus the number of snapshots for noncircular signals

In the second case, the root-mean-square error (RMSE) of the above algorithms is compared for noncircular wideband DOA estimation. The RMSE can be defined as

$$\mathrm{RMSE}_{\theta}=\sqrt{\frac{1}{K_{\mathrm{nc}}T}\sum_{n=1}^{T}\sum_{k=1}^{K_{\mathrm{nc}}}\sum_{i=1}^{P_k}\left(\widehat{\theta}_{ki,n}-\theta\right)^2}. \tag{23}$$

A group of two off-grid BPSK wideband signals impinges onto the four elements minimum-redundancy linear array located at $(0, d, 4d, 6d)$ from $(-10.5^\circ, 13.2^\circ)$. The noncircularity phase and noncircularity rate of the LOS signals are 50° and 1 respectively. The multipath propagation delay is $\iota_{12}=T_{\mathrm{c}}$, and the attenuation factor is $\rho_{12}=0.8e^{j57.2^\circ}$. Let SNR increase 10 dB gradually to $N=2000$. Other conditions remain unchanged; the results are shown in Figure 2A. Then, N is changed from 1000 to 5000, and the SNR is 0 dB. Other simulation parameters remain unchanged; the results are displayed in Figure 2B. Appendix B contains the CRB for wideband noncircular DOA estimation. The estimation accuracy of subspace-based algorithms degrades in low SNR because multipath delay and attenuation factors

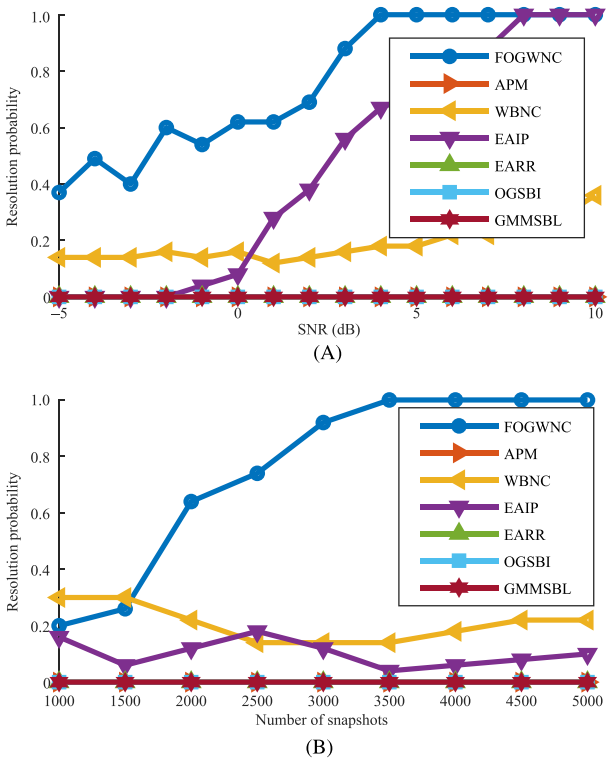

FIGURE 3 Resolution probability. (A) Resolution probability versus SNR for noncircular signals. (B) Resolution probability versus the number of snapshots for noncircular signals

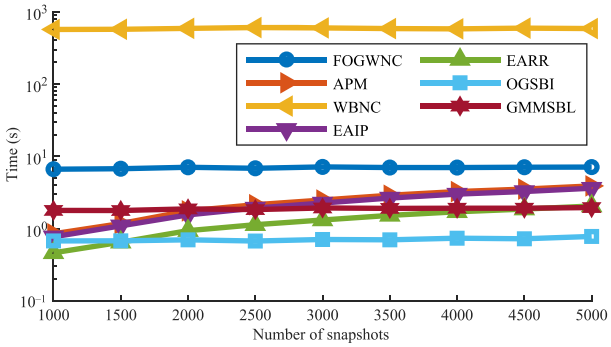

FIGURE 4 Cost time versus the number of snapshots

are not taken into account. FOGWNC has the highest precision for noncircular wideband sources among these algorithms in the given scenarios, as shown in Figure 2.

In the third case, the resolution probabilities of the above algorithms are compared to further illustrate the performance. A group of two off-grid BPSK wideband signals incident from $(0.1^\circ, 3.8^\circ)$. Two signals are resolved if both $|\widehat{\theta}_{11}-\theta_{11}|$ and $|\widehat{\theta}_{12}-\theta_{12}|$ are smaller 1°. First, the parameters are the same as that in Figure 2A; the results are shown in Figure 3A. The parameters are then the same as in Figure 2B, and the results are shown in Figure 3B. FOGWNC, followed by EAIP, has the best resolution probability among these algorithms, as shown in the results. Other methods cannot tell the difference between two signals that are too close together.

The computational cost of FOGWNC is considered in the last case. The convex optimization problems in the proposed algorithm can be solved by the CVX toolbox [38], and the main complexities of FOGWNC are $O(K_g^3)$. Figure 4 depicts the CPU time of the simulations in Figure 2B. The results show that FOGWNC takes longer to run than other algorithms but is much faster than WBNC.

5 | CONCLUSIONS

The off-grid-based algorithms for wideband noncircular DOA estimation were investigated in this paper. A novel algorithm called FOGWNC is developed using the focused operation. The presented algorithm outperforms existing noncircular wideband DOA estimators in low SNR, has the best resolution ability, and has the highest estimation accuracy, according to simulation results. This paper contributes to the advancement of SR theory's application in noncircular wideband DOA estimation.

ACKNOWLEDGMENTS

This research was funded in part by the Innovation Project of Science and Technology Commission of the Central Military Commission under Grant 19-HXXX-01-ZD-006-XXX-XX, in part by the National Key Laboratory Foundation under Grant 61424110302 and in part by the National Natural Science Foundation of China under Grant 61771015.

CONFLICT OF INTEREST

The authors declare that there are no conflicts of interest.

ORCID

Xiaoyu Zhang https://orcid.org/0000-0003-1187-8671
Haihong Tao https://orcid.org/0000-0002-4732-0015
Ziye Fang https://orcid.org/0000-0002-1638-6249
Jian Xie https://orcid.org/0000-0001-9654-064X

REFERENCES

1. P. Gounon, C. Adnet, and J. Galy, *Localization angulaire de signaux non circulaires*, Traitement du Signal. **15** (1998), no. 1, 17–23.
2. P. Chargé, Y. Wang, and J. Saillard, *A noncircular sources direction finding method using polynomial rooting*, Signal Process. **81** (2001), 1765–1770.
3. H. Abeida and J. P. Delmas, *MUSIC-like estimation of direction of arrival for noncircular sources*, IEEE Trans. Signal Process. **54** (2006), no. 7, 2678–2690.
4. F. Gao, A. Nallanathan, and Y. Wang, *Improved MUSIC under the coexistence of both circular and noncircular sources*, IEEE Trans. Signal Process. **56** (2008), no. 7, 3033–3038.
5. J. Liu, Z. Huang, and Y. Zhou, *Extended 2q-MUSIC algorithm for noncircular signals*, Signal Process. **88** (2008), no. 6, 1327–1339.
6. X. Gou, Z. Liu, and Y. Xu, *Biquaternion cumulant-MUSIC for DOA estimation of noncircular signals*, Signal Process **93** (2013), no. 4, 874–881.
7. Z. Liu, Z. Huang, Y. Zhou, and J. Liu, *Direction-of-arrival estimation of noncircular signals via sparse representation*, IEEE Trans. Aerosp. Electron. Syst. **48** (2012), no. 3, 2690–2698.
8. X. Yang, G. Li, and Z. Zheng, *DOA estimation of noncircular signal based on sparse representation*, Wirel. Pers. Commun. **82** (2015), no. 4, 2363–2375.
9. J. Cai, W. Liu, R. Zong, and B. Wu, *Sparse array extension for non-circular signals with subspace and compressive sensing based DOA estimation methods*, Signal Process. **145** (2018), 59–67.
10. R. Zheng, X. Xu, Z. Ye, T. Mahmud, J. Dai, and K. Shabir, *Sparse Bayesian learning for off-grid DOA estimation with Gaussian mixture priors when both circular and non-circular sources coexist*, Signal Process. **161** (2019), 124–135.
11. M. Doron, A. Weiss, and H. Messer, *Maximum-likelihood direction finding of wide-band sources*, IEEE Trans. Signal Process. **41** (1993), no. 1, 411–414.
12. P. Schultheiss and H. Messer, *Optimal and suboptimal broadband source location estimation*, IEEE Trans. Signal Process. **41** (1993), no. 9, 2752–2763.
13. M. Agrawal and S. Prasad, *DOA estimation of wideband sources using a harmonic source model and uniform linear array*, IEEE Trans. Signal Process. **47** (1999), no. 3, 619–629.
14. K. Buckley and L. Griffiths, *Broad-band signal-subspace spatial-spectrum (BASS-ALE) estimation*, IEEE Trans. Acoust., Speech, Signal Process. **36** (1988), no. 7, 953–964.
15. B. Yin, Y. Xu, Y. Huang, Y. Lu, and Z. Liu, *Direction finding for wideband source signals via steered effective projection*, IEEE Sens. J. **18** (2018), no. 2, 741–751.
16. S. Amirsoleimani and A. Olfat, *Wideband modal orthogonality: A new approach for broadband DOA estimation*, Signal Process. **176** (2020), 107696.
17. M. Wax, T. J. Shan, and T. Kailath, *Spatio-temporal spectral analysis by eigenstructure methods*, IEEE Trans. Acoust., Speech, Signal Process. **32** (1984), no. 4, 817–827.
18. H. Wang and M. Kaveh, *Coherent signal-subspace processing for the detection and estimation of angles of arrival of multiple wide-band sources*, IEEE Trans. Acoust., Speech, Signal Process. **33** (1985), no. 4, 823–831.
19. Y. Yoon, L. Kaplan, and J. McClellan, *TOPS: New DOA estimator for wideband signals*, IEEE Trans. Signal Process. **54** (2006), no. 6, 1977–1989.
20. Y. Bai, J. Li, Y. Wu, Q. Wang, and X. Zhang, *Weighted incoherent signal subspace method for DOA estimation on wideband colored signals*, IEEE Access. **7** (2019), 1224–1233.
21. H. Hung and M. Kaveh, *Focussing matrices for coherent signal-subspace processing*, IEEE Trans. Acoust., Speech, Signal Process. **36** (1988), no. 8, 1272–1281.
22. S. Valaee and P. Kabal, *Wideband array processing using a two-sided correlation transformation*, IEEE Trans. Signal Process. **43** (1995), no. 1, 160–172.
23. D. Feng, M. Bao, Z. Ye, L. Guan, and X. Li, *A novel wideband DOA estimator based on Khatri–Rao subspace approach*, Signal Process. **91** (2011), 2415–2419.
24. Z. Liu, Z. Huang, and Y. Zhou, *Direction-of-arrival estimation of wideband signals via covariance matrix sparse representation*, IEEE Trans. Signal Process. **59** (2011), no. 9, 4256–4270.
25. Q. Shen, W. Cui, W. Liu, S. Wu, Y. Zhang, and M. Amin, *Underdetermined wideband DOA estimation of off-grid sources employing the difference co-array concept*, Signal Process. **130** (2017), 299–304.
26. N. Hu, B. Sun, Y. Zhang, J. Dai, J. Wang, and C. Chang, *Underdetermined DOA estimation method for wideband signals using joint nonnegative sparse Bayesian learning*, IEEE Signal Process. Lett **24** (2017), no. 5, 535–539.
27. Y. Shi, X. Mao, C. Zhao, and Y. Liu, *Underdetermined DOA estimation for wideband signals via joint sparse signal reconstruction*, IEEE Signal Process. Lett. **26** (2019), no. 10, 1541–1545.
28. W. Cui, Q. Shen, W. Liu, and S. Wu, *Low complexity DOA estimation for wideband off-grid sources based on re-focused compressive sensing with dynamic dictionary*, IEEE J. Sel. Top. Signal Process. **13** (2019), no. 5, 918–930.
29. Q. Shen, W. Liu, W. Cui, S. Wu, Y. D. Zhang, and M. G. Amin, *Focused compressive sensing for underdetermined wideband DOA estimation exploiting high-order difference coarrays*, IEEE Signal Process. Lett. **24** (2017), no. 1, 86–90.
30. X. Zhang, H. Tao, J. Xie, and X. Jiang, *A novel wideband DOA estimation method based on a fast sparse frame*, IET Commun. **15** (2021), no. 7, 935–945.

31. J. Krolik and D. Swingler, *Multiple broad-band source location using steered covariance matrices*, IEEE Trans. Acoust., Speech, Signal Process. **37** (1989), no. 10, 1481–1494.
32. Y. Huang, Y. Xu, Y. Lu, and Z. Liu, *Envelope aligned inverse power scanning for direction of arrival estimation of circular and noncircular wideband source signals*, IET Microw. Antennas Propag. **12** (2018), no. 9, 1494–1503.
33. Y. Huang, Y. Lu, Y. Xu, and Z. Liu, *Direction-of-arrival estimation of circular and noncircular wideband source signals via augmented envelope alignment*, IEEE Sens. J. **13** (2019), no. 2, 1219–1230.
34. Y. Huang, Y. Xu, Y. Lu, and Z. Liu, *Aligned propagator scanning approach to DOA estimation of circular and noncircular wideband source signals*, IEEE Trans. Veh. Technol. **68** (2019), no. 2, 1702–1717.
35. Y. Yang, Z. Liu, Y. Xu, and J. Zhuang, *Cumulant-based biquaternion approach to direction finding of wideband signals*, IEEE Signal Commun. Lett. **24** (2020), no. 3, 630–634.
36. Z. Yang, L. Xie, and C. Zhang, *Off-grid direction of arrival estimation using sparse Bayesian inference*, IEEE Trans. Signal Process. **61** (2013), no. 1, 38–43.
37. A. Moffet, *Minimum-redundancy linear arrays*, IEEE Trans. Antennas Propag. **16** (1968), no. 2, 172–175.
38. M. Grant and S. Boyd, CVX: *Matlab Software for Disciplined Convex Programming*, 2008, Available from: http://cvxr.com/cvx
39. J. Delmas and H. Abeida, *Stochastic Cramer-Rao bound for noncircular signals with application to DOA estimation*, IEEE Trans. Signal Process. **52** (2004), no. 11, 3192–3199.

AUTHOR BIOGRAPHIES

Xiaoyu Zhang received the B.S. degree from the School of Electronic Engineering, Xidian University, Xi'an, China, in 2017. He is currently pursuing the Ph.D. degree with the National Laboratory of Radar Signal Processing, Xidian University. His research interests include array signal processing and compressive sensing.

Haihong Tao received the M.S. and Ph.D. degrees from the School of Electronic Engineering, Xidian University, Xi'an, China, in 2000 and 2004, respectively. She is currently a Professor with the School of Electronic Engineering, Xidian University. Her research interests include radar signal processing and array signal processing.

Ziye Fang received the B.S. degree from South China Normal University in 2016 and the M.S. degree from Shaanxi Normal University in 2019. She is currently pursuing the Ph.D. degree in Xidian University. Her research interests include compressive sensing and neural networks.

Jian Xie received his MS and PhD degrees from the School of Electronic Engineering, Xidian University, in 2012 and 2015, respectively. He is now an associate professor at Northwestern Polytechnical University. His research interests include antenna array processing and radar signal processing.

How to cite this article: X. Zhang, H. Tao, Z. Fang, and J. Xie, *Off-grid direction-of-arrival estimation for wideband noncircular sources*, ETRI Journal **45** (2023), 492–504. https://doi.org/10.4218/etrij.2021-0485

APPENDIX A: DERIVATION OF THE ERROR BOUND

Denote $a_{m,ki}$ and n_m as the mth elements of $\boldsymbol{a}(ki,l_r)$ and $\mathbf{N}[l_r,q]$, respectively. $x_{ki,q}$ is a simple expression for kith entry in $\mathbf{X}[l_r,q]$. We have

$$\begin{aligned}\widehat{\mathbf{R}}_{\mathrm{rc\_}m_1,m_2}&=\frac{1}{Q}\sum_{q=1}^{Q}\left(\sum_{k=1}^{K}\sum_{i=1}^{P_k}a_{m_1,ki}x_{ki,q}+n_{m_1}\right)\left(\sum_{k=1}^{K}\sum_{i=1}^{P_k}a^*_{m_2,ki}x^*_{ki,q}+n^*_{m_2}\right)\\&=\frac{1}{Q}\sum_{k=1}^{K}\sum_{i=1}^{P_k}\left(\sum_{q=1}^{Q}x^2_{ki,q}\right)a_{m_1,ki}a^*_{m_2,ki}\\&\quad+\underbrace{\frac{1}{Q}\sum_{q=1}^{Q}n_{m_1}n^*_{m_2}}_{\beta_{c\bar{m}_1,m_2}(1)}+\underbrace{\frac{1}{Q}\sum_{q=1}^{Q}\sum_{k=1}^{K}\sum_{i=1}^{P_k}a_{m_1,ki}x_{ki,q}n^*_{m_2}+\frac{1}{Q}\sum_{q=1}^{Q}\sum_{k=1}^{K}\sum_{i=1}^{P_k}a^*_{m_2,ki}x^*_{ki,q}n_{m_1}}_{\beta_{c\bar{m}_1,m_2}(2)}\\&\quad+\underbrace{\frac{1}{Q}\sum_{q=1}^{Q}\sum_{k_1=1}^{K}\sum_{\substack{k_2=1\\k_2i_2\neq k_1i_1}}^{K}\sum_{i_1=1}^{P_{k_1}}\sum_{i_2=1}^{P_{k_2}}a_{m_1,k_1i_1}a^*_{m_2,k_2i_2}x_{k_1i_1,q}x^*_{k_2i_2,q}}_{\beta_{c\bar{m}_1,m_2}(3)},\end{aligned}\tag{24}$$

$$\begin{aligned}\widehat{\mathbf{R}}_{\mathrm{rnc\_}m_1,m_2}&=\frac{1}{Q}\sum_{q=1}^{Q}\left(\sum_{k=1}^{K}\sum_{i=1}^{P_k}a_{m_1,ki}x_{ki,q}+n_{m_1}\right)\left(\sum_{k=1}^{K}\sum_{i=1}^{P_k}a_{m_2,ki}x_{ki,q}+n_{m_2}\right)\\&=\frac{1}{Q}\sum_{k=1}^{K}\sum_{i=1}^{P_k}\left(\sum_{q=1}^{Q}x^2_{ki,q}\right)a_{m_1,ki}a_{m_2,ki}\\&\quad+\underbrace{\frac{1}{Q}\sum_{q=1}^{Q}n_{m_1}n_{m_2}}_{\beta_{\mathrm{nc}\bar{m}_1,m_2}(1)}+\underbrace{\frac{1}{Q}\sum_{q=1}^{Q}\sum_{k=1}^{K}\sum_{i=1}^{P_k}a_{m_1,ki}x_{ki,q}n_{m_2}+\frac{1}{Q}\sum_{q=1}^{Q}\sum_{k=1}^{K}\sum_{i=1}^{P_k}a_{m_2,ki}x_{ki,q}n_{m_1}}_{\beta_{\mathrm{nc}\bar{m}_1,m_2}(2)}\\&\quad+\underbrace{\frac{1}{Q}\sum_{q=1}^{Q}\sum_{k_1=1}^{K}\sum_{\substack{k_2=1\\k_2i_2\neq k_1i_1}}^{K}\sum_{i_1=1}^{P_{k_1}}\sum_{i_2=1}^{P_{k_2}}a_{m_1,k_1i_1}a_{m_2,k_2i_2}x_{k_1i_1,q}x_{k_2i_2,q}}_{\beta_{\mathrm{nc}\bar{m}_1,m_2}(3)}.\end{aligned}\tag{25}$$

It is obvious that the first terms of $\widehat{\mathbf{R}}_{\mathrm{rc\_}m_1,m_2}$ and $\widehat{\mathbf{R}}_{\mathrm{rnc\_}m_1,m_2}$ are the signal component and the other three terms are the perturbation, that is,

$$\begin{aligned}\beta_{\mathrm{c}_{m_1},m_2}&=\beta_{\mathrm{c}_{m_1},m_2}(1)+\beta_{\mathrm{c}_{m_1},m_2}(2)+\beta_{\mathrm{c}_{m_1},m_2}(3),\\\beta_{\mathrm{nc\_}m_1,m_2}&=\beta_{\mathrm{nc\_}m_1,m_2}(1)+\beta_{\mathrm{nc\_}m_1,m_2}(2)+\beta_{\mathrm{nc\_}m_1,m_2}(3).\end{aligned}\tag{26}$$

Taking advantage of the independence between signal and noise, the variances of perturbation can be deduced as

$$\begin{aligned}&\mathrm{E}\left\{\beta_{\mathrm{c}_{m_1},m_2}\beta^*_{\mathrm{c}_{m_1},m_2}\right\}=\sum\nolimits_{n=1}^{3}\mathrm{E}\left\{\beta_{\mathrm{c}_{m_1},m_2}(n)\beta^*_{\mathrm{c}_{m_1},m_2}(n)\right\}\\&=\frac{1}{Q}\left\{\overline{\sigma}^4+2\overline{\sigma}^2\sum_{k=1}^{K}\sum_{i=1}^{P_k}\overline{\gamma}_{\mathrm{c}}(ki)+\sum_{k_1=1}^{K}\sum_{k_2=1}^{K}\sum_{i_1=1}^{P_{k_1}}\sum_{i_2=1}^{P_{k_2}}\overline{\gamma}_{\mathrm{c}}(k_1i_1)\overline{\gamma}_{\mathrm{c}}(k_2i_2)\right.\\&\quad\left.+\sum_{k_1=1}^{K}\sum_{k_2=1}^{K}\sum_{i_1=1}^{P_{k_1}}\sum_{i_2=1}^{P_{k_2}}a_{m_1,k_1i_1}a^*_{m_2,k_1i_1}a^*_{m_1,k_2i_2}a_{m_2,k_2i_2}\overline{\gamma}_{\mathrm{nc}}(k_1i_1)\overline{\gamma}^*_{\mathrm{nc}}(k_2i_2)\right\},\end{aligned}\tag{27}$$

where $\sum_{k_1=1}^{K}\sum_{\substack{k_2=1\\k_2i_2\neq k_1i_1}}^{K}$ denotes the double sum over k_1,k_2 with $k_2i_2\neq k_1i_1$.

$$
\begin{aligned}
&\mathrm{E}\left\{\beta_{\mathrm{nc}\_m_1,m_2}\beta^*_{\mathrm{nc}\_m_1,m_2}\right\} \\
&= \sum\nolimits_{n=1}^{3} E\left\{\beta_{\mathrm{nc}\_m_1,m_2}(n)\beta^*_{\mathrm{nc}\_m_1,m_2}(n)\right\} \\
&= \frac{1}{Q}\left\{\overline{\sigma}^4 + \overline{\sigma}^4\delta(m_1-m_2) + 2\overline{\sigma}^2\sum_{k=1}^{K}\sum_{i=1}^{P_k}\overline{\gamma}_{\mathrm{c}}(ki) + 2\overline{\sigma}^2\delta(m_1-m_2)\sum_{k=1}^{K}\sum_{i=1}^{P_k}\overline{\gamma}_{\mathrm{c}}(ki)\right. \\
&\quad \left. + \sum_{k_1=1}^{K}\sum_{k_2=1}^{K}\sum_{\substack{i_1=1\\ k_2i_2\neq k_1i_1}}^{P_{k_1}}\sum_{i_2=1}^{P_{k_2}}\overline{\gamma}_{\mathrm{c}}(k_1i_1)\overline{\gamma}_{\mathrm{c}}(k_2i_2) + \sum_{k_1=1}^{K}\sum_{k_2=1}^{K}\sum_{\substack{i_1=1\\ k_2i_2\neq k_1i_1}}^{P_{k_1}}\sum_{i_2=1}^{P_{k_2}} a_{m_1,k_1i_1}a^*_{m_2,k_1i_1}a^*_{m_1,k_2i_2}a_{m_2,k_2i_2}\overline{\gamma}_{\mathrm{nc}}(k_1i_1)\overline{\gamma}^*_{\mathrm{nc}}(k_2i_2)\right\}.
\end{aligned} \tag{28}
$$

Then, the mean square value of the covariance observation vector with the reference frequency bin can be formulated as

$$
\begin{aligned}
\mathrm{E}\left\{\|\boldsymbol{\beta}_{\mathrm{c}}\|_2^2\right\} &= \sum_{m_1=1}^{M}\sum_{\substack{m_2=1\\ m_2\neq m_1}}^{M} E\left\{\beta_{\mathrm{c}_{m_1},m_2}\beta^*_{\mathrm{c}_{m_1},m_2}\right\} \\
&= \frac{M(M-1)}{Q}\cdot\left(\overline{\sigma}^4 + 2\overline{\sigma}^2\sum_{k=1}^{K}\sum_{i=1}^{P_k}\overline{\gamma}_{\mathrm{c}}(ki) + \sum_{k_1=1}^{K}\sum_{k_2=1}^{K}\sum_{\substack{i_1=1\\ k_2i_2\neq k_1i_1}}^{P_{k_1}}\sum_{i_2=1}^{P_{k_2}}\overline{\gamma}_{\mathrm{c}}(k_1i_1)\overline{\gamma}_{\mathrm{c}}(k_2i_2)\right) \\
&\quad + \frac{1}{Q}\cdot\sum_{m_1=1}^{M}\sum_{\substack{m_2=1\\ m_2\neq m_1}}^{M}\sum_{k_1=1}^{K}\sum_{k_2=1}^{K}\sum_{\substack{i_1=1\\ k_2i_2\neq k_1i_1}}^{P_{k_1}}\sum_{i_2=1}^{P_{k_2}} a_{m_1,k_1i_1}a_{m_2,k_1i_1}a^*_{m_1,k_2i_2}a^*_{m_2,k_2i_2}\overline{\gamma}_{\mathrm{nc}}(k_1i_1)\overline{\gamma}^*_{\mathrm{nc}}(k_2i_2) \\
&= \frac{M(M-1)}{Q}\left(\overline{\sigma}^2 + \sum_{k=1}^{K}\sum_{i=1}^{P_k}\overline{\gamma}_{\mathrm{c}}(ki)\right)^2 - \frac{M(M-1)}{Q}\sum_{k=1}^{K}\sum_{i=1}^{P_k}\overline{\gamma}_{\mathrm{c}}^2(ki) \\
&\quad + \frac{1}{Q}\sum_{m_1=1}^{M}\sum_{\substack{m_2=1\\ m_2\neq m_1}}^{M}|\mathbf{R}_{\mathrm{rnc}\_m_1,m_2}|^2 - \frac{M(M-1)}{Q}\sum_{k=1}^{K}\sum_{i=1}^{P_k}\overline{\gamma}_{\mathrm{nc}}^2(ki),
\end{aligned} \tag{29}
$$

$$
\begin{aligned}
&\mathrm{E}\left\{\|\boldsymbol{\beta}_{\mathrm{nc}}\|_2^2\right\}\\
&=\sum_{m_1=1}^{M}\sum_{m_2=1}^{M}E\left\{\beta_{nc_{m_1},m_2}\beta^{*}_{\mathrm{nc}_{m_1},m_2}\right\}\\
&=\frac{M^2}{Q}\left[\left(\overline{\sigma}^4(1+\delta(m_1-m_2))+\sum_{k_1=1}^{K}\sum_{k_2=1}^{K}\sum_{\substack{i_1=1\\ k_2i_2\neq k_1i_1}}^{P_{k_1}}\sum_{i_2=1}^{P_{k_2}}\overline{\gamma}_{\mathrm{c}}(k_1i_1)\overline{\gamma}_{\mathrm{c}}(k_2i_2)+2\overline{\sigma}^2(1+\delta(m_1-m_2))\sum_{k=1}^{K}\sum_{i=1}^{P_k}\overline{\gamma}_{\mathrm{c}}(ki)\right)\right.\\
&\quad\left.+\frac{1}{Q}\sum_{k_1=1}^{K}\sum_{k_2=1}^{K}\sum_{\substack{i_1=1\\ k_2i_2\neq k_1i_1}}^{P_{k_1}}\sum_{i_2=1}^{P_{k_2}}a_{m_1,k_1i_1}a^{*}_{m_2,k_1i_1}a^{*}_{m_1,k_2i_2}a_{m_2,k_2i_2}\overline{\gamma}_{\mathrm{nc}}(k_1i_1)\overline{\gamma}^{*}_{\mathrm{nc}}(k_2i_2)\right]\\
&=\frac{M(M+1)}{Q}\left(\overline{\sigma}^2+\sum_{k=1}^{K}\sum_{i=1}^{P_k}\overline{\gamma}_{\mathrm{c}}(ki)\right)^2-\frac{M^2}{Q}\sum_{k=1}^{K}\sum_{i=1}^{P_k}\overline{\gamma}_{\mathrm{c}}^2(ki)\\
&\quad-\frac{M}{Q}\left(\sum_{k=1}^{K}\sum_{i=1}^{P_k}\overline{\gamma}_{\mathrm{c}}(ki)\right)^2+\frac{1}{Q}\sum_{m_1=1}^{M}\sum_{m_2=1}^{M}\left|\boldsymbol{R}_{\mathrm{rc}_{m_1},m_2}\right|^2-\frac{M^2}{Q}\sum_{k=1}^{K}\sum_{i=1}^{P_k}\overline{\gamma}_{\mathrm{c}}^2(ki)\\
&=\frac{M(M+1)}{Q}\left(\overline{\sigma}^2+\sum_{k=1}^{K}\sum_{i=1}^{P_k}\overline{\gamma}_{\mathrm{c}}(ki)\right)^2-\frac{2M^2}{Q}\sum_{k=1}^{K}\sum_{i=1}^{P_k}\overline{\gamma}_{\mathrm{c}}^2(ki)+\frac{1}{Q}\sum_{m_1=1}^{M}\sum_{\substack{m_2=1\\ m_2\neq m_1}}^{M}|\mathbf{R}_{\mathrm{rc\_}m_1,m_2}|^2.
\end{aligned}
\tag{30}
$$

The error can be set as

$$
\varepsilon_{\mathrm{c}}=\mu_{\mathrm{c}}\left[\mathrm{E}\left\{\|\boldsymbol{\beta}_{\mathrm{c}}\|_2^2\right\}\right]^{\frac{1}{2}},\varepsilon_{\mathrm{nc}}=\mu_{\mathrm{nc}}\left[\mathrm{E}\left\{\|\boldsymbol{\beta}_{\mathrm{nc}}\|_2^2\right\}\right]^{\frac{1}{2}}. \tag{31}
$$

APPENDIX B: CRAMER–RAO BOUND OF WIDEBAND NONCIRCULAR DOA ESTIMATION

Denote the $K+3KL+L$ dimensional unknown parameter vector:

$$
\boldsymbol{\xi}=\left[\boldsymbol{\theta}^{\mathrm{T}},\breve{\boldsymbol{\gamma}}_{\mathrm{c}}^{\mathrm{T}},\breve{\boldsymbol{\gamma}}_{\mathrm{nc}}^{\mathrm{T}},\boldsymbol{\sigma}^{\mathrm{T}}\right]^{\mathrm{T}}, \tag{32}
$$

where

$$
\begin{aligned}
\breve{\boldsymbol{\gamma}}_{\mathrm{c}}&=\left[\boldsymbol{\gamma}_{\mathrm{c}}^{\mathrm{T}}[1],\boldsymbol{\gamma}_{\mathrm{c}}^{\mathrm{T}}[2],...,\boldsymbol{\gamma}_{\mathrm{c}}^{\mathrm{T}}[\mathrm{L}]\right]^{\mathrm{T}}\\
\breve{\boldsymbol{\gamma}}_{\mathrm{nc}}&=\left[\Re\left(\boldsymbol{\gamma}_{\mathrm{nc}}^{\mathrm{T}}[1]\right),\Im\left(\boldsymbol{\gamma}_{\mathrm{nc}}^{\mathrm{T}}[1]\right),...,\Re\left(\boldsymbol{\gamma}_{\mathrm{nc}}^{\mathrm{T}}[L]\right),\Im\left(\boldsymbol{\gamma}_{\mathrm{nc}}^{\mathrm{T}}[L]\right)\right]^{\mathrm{T}}\\
\boldsymbol{\sigma}&=\left[\sigma_1^2,\sigma_2^2,...,\sigma_L^2\right]^{T}.
\end{aligned}
\tag{33}
$$

Unlike the circular signals, the pseudo covariance matrix also contains information about directions and power. The augmented covariance matrix of each frequency bin can be formulated as

$$
\breve{\boldsymbol{R}}[l]=\begin{bmatrix}\mathbf{R}_{\mathrm{c}}[l] & \mathbf{R}_{\mathrm{nc}}[l]\\ \mathbf{R}_{\mathrm{nc}}^{*}[l] & \mathbf{R}_{\mathrm{c}}^{*}[l]\end{bmatrix}. \tag{34}
$$

According to the Slepian–Bangs formula for noncircular sources [39], the element at ith row and jth column of the Fisher information matrix (FIM) can be denoted as

$$
\begin{aligned}
\mathbf{FIM}_{i,j}=\frac{Q}{2}\sum\nolimits_{l=1}^{L}&\left\{\left(\breve{\mathbf{R}}^{\mathrm{T}}[l]\otimes\breve{\mathbf{R}}[l]\right)^{-\frac{1}{2}}\frac{\partial\breve{\boldsymbol{r}}(l)}{\partial\boldsymbol{\xi}_i}\right\}^{\mathrm{H}}\\
&\cdot\left\{\left(\breve{\mathbf{R}}^{\mathrm{T}}[l]\otimes\breve{\mathbf{R}}[l]\right)^{-\frac{1}{2}}\frac{\partial\breve{\boldsymbol{r}}(l)}{\partial\boldsymbol{\xi}_j}\right\},
\end{aligned}
\tag{35}
$$

where $\breve{\mathbf{r}}[l]=\mathrm{vec}\left(\breve{\mathbf{R}}[l]\right)$. It is difficult to directly calculate the derivative of $\breve{\mathbf{r}}[l]$, and the vectorization of each part of $\breve{\mathbf{R}}[l]$ may be separated $\breve{\mathbf{r}}[l]$ to facilitate the derivation. Define a $4M^2\times4M^2$ dimensional permutation matrix as

$$
\boldsymbol{\Xi}=\left[\mathbf{I}_2\otimes\left(\sum\nolimits_{m=1}^{M}\sum\nolimits_{i=1}^{2}\mathbf{F}_{m,j}\otimes\mathbf{F}_{m,j}^{\mathrm{T}}\right)\otimes\mathbf{I}_M\right], \tag{36}
$$

where $\mathbf{F}_{m,j}$ is a $M \times 2$ dimensional matrix, the element at ith row and jth column of $\mathbf{F}_{m,j}$ is 1, and the other elements are 0. Denote $\mathbf{r}_{\mathrm{c}}[l] = \mathrm{vec}(\mathbf{R}_{\mathrm{c}}[l])$ and $\mathbf{r}_{\mathrm{nc}}[l] = \mathrm{vec}(\mathbf{R}_{\mathrm{nc}}[l])$, $\breve{\mathbf{r}}[l]$ can be rewritten as

$$\breve{\mathbf{r}}[l] = \boldsymbol{\Xi}\left[\mathbf{r}_{\mathrm{c}}^{\mathrm{T}}[l], \mathbf{r}_{\mathrm{nc}}^{\mathrm{H}}[l], \mathbf{r}_{\mathrm{nc}}^{\mathrm{T}}[l], \mathbf{r}_{\mathrm{c}}^{\mathrm{H}}[l]\right]^{\mathrm{T}}. \tag{37}$$

The derivatives of $\mathbf{r}_{\mathrm{c}}[l]$ and $\mathbf{r}_{\mathrm{nc}}[l]$ can be formulated as

$$\begin{aligned}
&\frac{\partial \mathbf{r}_{\mathrm{c}}[l]}{\partial \boldsymbol{\theta}^{\mathrm{T}}} = \mathbf{A}_{\mathrm{c}}'[l]\mathrm{diag}(\boldsymbol{\gamma}_{\mathrm{c}}[l]), \frac{\partial \mathbf{r}_{\mathrm{c}}[l]}{\partial \breve{\boldsymbol{\gamma}}_{\mathrm{nc}}^{\mathrm{T}}} = \mathbf{O}_{M^2 \times KL} \\
&\frac{\partial \mathbf{r}_{\mathrm{c}}[l]}{\partial \breve{\boldsymbol{\gamma}}_{\mathrm{c}}^{\mathrm{T}}} = \left[\mathbf{O}_{M^2 \times K}, \ldots, \underbrace{\mathbf{A}_{\mathrm{c}}[l]}_{\text{the } l\text{th block}}, \ldots, \mathbf{O}_{M^2 \times K}\right] \\
&\frac{\partial \mathbf{r}_{\mathrm{c}}[l]}{\partial \boldsymbol{\sigma}^{\mathrm{T}}} = \left[\mathbf{O}_{M^2 \times 1}, \ldots, \underbrace{i_{M^2}}_{\text{the } l\text{th block}}, \ldots, \mathbf{O}_{M^2 \times 1}\right] \\
&\frac{\partial \mathbf{r}_{\mathrm{nc}}[l]}{\partial \boldsymbol{\theta}^{\mathrm{T}}} = \mathbf{A}_{\mathrm{nc}}'[l]\mathrm{diag}(\boldsymbol{\gamma}_{\mathrm{nc}}[l]), \frac{\partial \mathbf{r}_{\mathrm{nc}}[l]}{\partial \breve{\boldsymbol{\gamma}}_{\mathrm{c}}^{\mathrm{T}}} = \mathbf{O}_{M^2 \times KL}, \\
&\frac{\partial \mathbf{r}_{\mathrm{nc}}[l]}{\partial \breve{\boldsymbol{\gamma}}_{\mathrm{nc}}^{\mathrm{T}}} = \left[\mathbf{O}_{M^2 \times 2K}, \ldots, \underbrace{\mathbf{A}_{\mathrm{nc}}[l]\boldsymbol{\Psi}}_{\text{the } l\text{th block}}, \ldots, \mathbf{O}_{M^2 \times 2K}\right], \frac{\partial \mathbf{r}_{\mathrm{nc}}[l]}{\partial \boldsymbol{\sigma}^{\mathrm{T}}} = \mathbf{O}_{M^2 \times L},
\end{aligned} \tag{38}$$

The definition of $\mathbf{A}_{\mathrm{c}}[l]$, $\mathbf{A}_{\mathrm{nc}}[l]$,$\mathbf{A}_{\mathrm{c}}'[l]$, and $\mathbf{A}_{\mathrm{nc}}'[l]$ can be found in (8) and (13), $\boldsymbol{\gamma}_{\mathrm{nc}}^{\mathrm{T}}[l] = \boldsymbol{\Psi}\left[\Re\left(\boldsymbol{\gamma}_{\mathrm{nc}}^{\mathrm{T}}[l]\right), \Im\left(\boldsymbol{\gamma}_{\mathrm{nc}}^{\mathrm{T}}[l]\right)\right]^{\mathrm{T}}$ Let $\mathbf{W}_l = \left(\breve{\mathbf{R}}^{\mathrm{T}}[l] \bigotimes \breve{\mathbf{R}}[l]\right)^{-\frac{1}{2}}$, the FIM can be transformed as

$$\mathbf{FIM} = \frac{Q}{2}\begin{bmatrix} \mathbf{G}_{\theta}^{\mathrm{H}}\mathbf{G}_{\theta} & \mathbf{G}_{\theta}^{\mathrm{H}}\mathbf{G}_{p} \\ \mathbf{G}_{p}^{\mathrm{H}}\mathbf{G}_{\theta} & \mathbf{G}_{p}^{\mathrm{H}}\mathbf{G}_{p} \end{bmatrix}, \tag{39}$$

where

$$\begin{aligned}
&\mathbf{G}_{\theta} = \widetilde{\mathbf{W}}(\boldsymbol{I}_L \bigotimes \boldsymbol{\Xi})\widetilde{\mathbf{D}}_{\theta}, \mathbf{G}_{p} = \widetilde{\mathbf{W}}(\mathbf{I}_L \bigotimes \boldsymbol{\Xi})\widetilde{\mathbf{D}}_{p} \\
&\widetilde{\mathbf{W}} = \mathrm{blkdiag}(\mathbf{W}_1, \mathbf{W}_2, \ldots, \mathbf{W}_L) \\
&\widetilde{\mathbf{D}}_{\theta} = \left[\mathbf{D}_{\theta}^{\mathrm{T}}[1], \mathbf{D}_{\theta}^{\mathrm{T}}[2], \ldots, \mathbf{D}_{\theta}^{\mathrm{T}}[L]\right]^{\mathrm{T}}, \widetilde{\mathbf{D}}_{p} = \left[\widetilde{\mathbf{D}}_{\mathrm{c}}, \widetilde{\mathbf{D}}_{\mathrm{nc}}, \widetilde{\mathbf{D}}_{\sigma}\right] \\
&\mathbf{D}_{\theta}[l] = \left[\left(\frac{\partial \mathbf{r}_{\mathrm{c}}[l]}{\partial \boldsymbol{\theta}^{\mathrm{T}}}\right)^{\mathrm{T}}, \left(\frac{\partial \mathbf{r}_{\mathrm{nc}}^{*}[l]}{\partial \boldsymbol{\theta}^{\mathrm{T}}}\right)^{\mathrm{T}}, \left(\frac{\partial \mathbf{r}_{\mathrm{nc}}[l]}{\partial \boldsymbol{\theta}^{H}}\right)^{\mathrm{T}}, \left(\frac{\partial \mathbf{r}_{\mathrm{c}}^{*}[l]}{\partial \boldsymbol{\theta}^{\mathrm{T}}}\right)^{\mathrm{T}}\right]^{\mathrm{T}} \\
&\widetilde{\mathbf{D}}_{\mathrm{c}} = \left[\boldsymbol{D}_{c}^{T}[1], \boldsymbol{D}_{c}^{T}[2], \ldots, \boldsymbol{D}_{c}^{T}[L]\right]^{\mathrm{T}} \\
&\mathbf{D}_{\mathrm{c}}[l] = \left[\left(\frac{\partial \mathbf{r}_{\mathrm{c}}[l]}{\partial \breve{\boldsymbol{\gamma}}_{\mathrm{c}}^{\mathrm{T}}}\right)^{\mathrm{T}}, \left(\frac{\partial \mathbf{r}_{\mathrm{nc}}^{*}[l]}{\partial \breve{\boldsymbol{\gamma}}_{\mathrm{c}}^{\mathrm{T}}}\right)^{\mathrm{T}}, \left(\frac{\partial \mathbf{r}_{\mathrm{nc}}[l]}{\partial \breve{\boldsymbol{\gamma}}_{\mathrm{c}}^{\mathrm{T}}}\right)^{\mathrm{T}}, \left(\frac{\partial \mathbf{r}_{\mathrm{c}}^{*}[l]}{\partial \breve{\boldsymbol{\gamma}}_{\mathrm{c}}^{\mathrm{T}}}\right)^{\mathrm{T}}\right]^{\mathrm{T}} \\
&\widetilde{\mathbf{D}}_{\mathrm{nc}} = \left[\mathbf{D}_{\mathrm{nc}}^{\mathrm{T}}[1], \mathbf{D}_{\mathrm{nc}}^{\mathrm{T}}[2], \ldots, \mathbf{D}_{\mathrm{nc}}^{\mathrm{T}}[L]\right]^{\mathrm{T}} \\
&\mathbf{D}_{\mathrm{nc}}[l] = \left[\left(\frac{\partial \mathbf{r}_{\mathrm{c}}[l]}{\partial \breve{\boldsymbol{\gamma}}_{\mathrm{nc}}^{\mathrm{T}}}\right)^{\mathrm{T}}, \left(\frac{\partial \mathbf{r}_{\mathrm{nc}}^{*}[l]}{\partial \breve{\boldsymbol{\gamma}}_{\mathrm{nc}}^{\mathrm{T}}}\right)^{\mathrm{T}}, \left(\frac{\partial \mathbf{r}_{\mathrm{nc}}[l]}{\partial \breve{\boldsymbol{\gamma}}_{\mathrm{nc}}^{\mathrm{T}}}\right)^{\mathrm{T}}, \left(\frac{\partial \mathbf{r}_{\mathrm{c}}^{*}[l]}{\partial \breve{\boldsymbol{\gamma}}_{\mathrm{nc}}^{\mathrm{T}}}\right)^{\mathrm{T}}\right]^{\mathrm{T}} \\
&\widetilde{\mathbf{D}}_{\sigma} = \left[\mathbf{D}_{\sigma}^{\mathrm{T}}[1], \mathbf{D}_{\sigma}^{\mathrm{T}}[2], \ldots, \mathbf{D}_{\sigma}^{\mathrm{T}}[L]\right]^{\mathrm{T}} \\
&\mathbf{D}_{\sigma}[l] = \left[\left(\frac{\partial \mathbf{r}_{\mathrm{c}}[l]}{\partial \boldsymbol{\sigma}^{\mathrm{T}}}\right)^{\mathrm{T}}, \left(\frac{\partial \mathbf{r}_{\mathrm{nc}}^{*}[l]}{\partial \boldsymbol{\sigma}^{\mathrm{T}}}\right)^{\mathrm{T}}, \left(\frac{\partial \mathbf{r}_{\mathrm{nc}}[l]}{\partial \boldsymbol{\sigma}^{\mathrm{T}}}\right)^{\mathrm{T}}, \left(\frac{\partial \mathbf{r}_{\mathrm{c}}^{*}[l]}{\partial \boldsymbol{\sigma}^{\mathrm{T}}}\right)^{\mathrm{T}}\right]^{\mathrm{T}}
\end{aligned} \tag{40}$$

Using the matrix inversion lemma, the CRB matrix can be formulated as

$$\mathbf{CRB}(\boldsymbol{\theta}) = \frac{2}{Q}\left(\mathbf{G}_{\theta}^{\mathrm{H}}\Pi_{\mathbf{G}_p}^{\perp}\mathbf{G}_{\theta}\right)^{-1}, \tag{41}$$

where

$$\Pi_{\mathbf{G}_p}^{\perp} = \mathbf{I}_{4M^2L} - \mathbf{G}_{p}\left(\mathbf{G}_{p}^{\mathrm{H}}\mathbf{G}_{p}\right)^{-1}\mathbf{G}_{p}^{H}. \tag{42}$$